

Final

Two-step development of geomagnetic storms

Y. Kamide¹, N. Yokoyama¹, W. Gonzalez^{1,2}, B. T. Tsurutani³, A. Brekke⁴, and S. Masuda¹

¹Solar-Terrestrial Environment Laboratory, Nagoya University, Toyokawa, Aichi 442, Japan

²Instituto Nacional de Pesquisas Espaciais, Postal 515, 12200 São José dos Campos, Sao Paulo, Brazil

³Jet Propulsion Laboratory, California Institute of Technology, Pasadena, CA 91109

⁴Auroral Observatory, University of Tromsø, Tromsø N-9037, Norway

Submitted to the Journal of Geophysical Research
As a Brief Report

May 30, 1997

Abstract. By using the *Dst* index, more than 1200 geomagnetic storms, from weak to intense, spanning over three solar cycles have statistically been examined, Data of the interplanetary magnetic field (IMF) and the solar wind have also been referred to. It is found that for more than 50% of intense magnetic storms, the main phase undergoes a two-step growth in the ring current field. That is, before the ring current has decayed significantly to the pre-storm level, a new major particle injection occurs, bringing in a further development of the ring current and making *Dst* grow a second time. Thus intense magnetic storms may often be the result of two closely-spaced moderate storms. The corresponding signature in the interplanetary medium is the arrival of double-structured southward IMF at the magnetosphere.

1. Introduction

In view of the increasingly wide recognition of the importance of Space Weather research in the scientific community, studies of geomagnetic storms have recently been revived [e.g., *Knipp et al.*, 1996]. The main objective of the Space Weather program is to understand the causes of magnetic storms in the solar/interplanetary medium and to trace energy flow associated with storms from the sun to the Earth's upper atmosphere. The present paper addresses the following major questions: Quantitatively, what magnetospheric parameter represents the intensity of magnetic storms; how one can define their strength on the basis of available data; and what parameters in the solar wind best determine how intense the upcoming magnetic storms will be.

Because of the close theoretical relationship between the total energy of ring current particles and the geomagnetic *Dst* index [*Dessler and Parker*, 1959; *Sckopke*, 1966; *Siscoe*, 1970], the minimum *Dst* value at the main phase of magnetic storms has customarily been used extensively in the literature [see *Joselyn and Tsurutani*, 1990]. In their extensive statistical study, *Sugiura and Chapman [1960]* divided magnetic storms into three categories in terms of the peak *Dst* value: weak, moderate, and intense storms. In that "classical" study, they identified magnetic storms on the basis of the existence of storm sudden commencements (SSCs), thus excluding the so-called gradual storms. In more recent studies, *Taylor et al. [1994]* and *Loewe and Pröls [1997]* have conducted statistical studies of geomagnetic storms in which *Dst* variations were compared with auroral electrojet activity, as well as with their interplanetary y causes. In those studies, they have taken essentially the same approach as *Sugiura and Chapman*, where the variability in duration for different storms was obscured in their averaging process.

In going through several published papers, however, we noticed that intense magnetic storms often develop in two-steps during the main phase [e.g., *Tsurutani et al.*, 1988]. It is of great interest to examine how often the ring current during magnetic

storms develops in such a two-step fashion, and if the percentage is not negligible, to look for the corresponding signatures in the solar wind and to discuss possible magnetospheric processes.

2. Procedure

A total of 1252 geomagnetic storms were identified for the period from 1957 to 1991, covering nearly three solar cycles. The entire dataset was grouped into three classes: weak ($Dst_{\min} > -50$ nT), moderate ($-50 > Dst_{\min} > -100$ nT), and intense ($Dst_{\min} < -100$ nT) magnetic storms, according to the magnitude of the storms, which was defined with the peak Dst values. Eyeball inspection of Dst was first employed to identify periods of magnetic storms. This was necessary because we did not wish to miss gradual storms that commence without a clear indication of SSC [Akasofu, 1965]. There was no indication for any clear relationship between the intensity of magnetic storms and whether storms commenced with or without SSCs.

We further classified each of the three classes of geomagnetic storms into two types, Type 1 and Type 2, according to how Dst reaches the peak through the main phase. Figure 1 shows schematically these two types of geomagnetic storms. Type 1 represents a “normal” magnetic storm that consists of the main phase and the subsequent recovery phase. During the main phase, the magnetic field on the Earth’s surface is significantly depressed. This depression is caused by an enhancement of the trapped particle population in the magnetosphere and thus by the (proton) ring current flowing westward. This sequence is at times preceded by the initial phase during which Dst shows a positive change responding to a pressure increase in the solar wind.

On the other hand, Type 2 is for a magnetic storm which has a two-step increase in the ring current field. To differentiate properly this type from Type 1, several parameters are introduced. Most importantly, the following two conditions are required:

(1) The first decrease in Dst must be subsided, i.e., $A > C > 0$ nT. C quantifies how much the first intensification in Dst has recovered before the second intensification commences; if $C/A > 0.9$, it were not a Type 2 storm, but simply a Type 1 storm having the A magnitude.

(2) The two peaks in Dst must be separated by more than three hours, $T_+ - Y > 3$ hrs. This condition was employed in order not to include cases where the Dst magnitude apparently decreases, caused by such substorm effects as the so-called current wedge, not by a true decrease in the storm-time ring current. (We note, however, that there are cases where two steps are closely spaced; these will be missed in the present study.)

It is easy to see, as an extreme case, that if $T = 0$ and $C = 0$, Type 2 becomes Type 1, whose intensity is $A + B$. We admit that even with these quantitative criteria, there are a number of “uncertain” magnetic storms in our dataset. The corresponding data of the AE indices and the IMF/solar wind have also been examined, whenever they were available.

3. Results

Figure 2 shows two typical examples of Type 2 storms. Two peaks in Dst (labeled as I and II) in the magnetic storm shown in Figure 2a are separated by only 4 hours, while those in Figure 2b are separated by 7 hours. This difference in separation time is also clearly identified in the corresponding B_z component of the IMF, although both cases include many fluctuations in the IMF data. It is interesting to point out that the Figure 2b case is a $C=0$ magnetic storm.

Table 1 summarizes statistics. Two points of interest are noted: First, more than 50% of all magnetic storms are found to go through two steps in Dst during the main phase. Second, the percentage of Type 2 occurrence increases statistically as the peak intensity $I > sI$ increases. That is, about 6796 of intense storms have the two-step growth and a relatively simple growth in Dst can be seen only in less than 30% of all storms.

For each of the 1252 magnetic storms, we have defined the main and recovery phases. Time 0 is defined as the time when Dst crosses zero, and the end of a storm is taken as the time when Dst recovers to one-tenth the level of its peak value. After defining these times, i.e., the start, peak and end, a superposed-epochal study is conducted to attempt to identify major characteristics common to different magnetic storms. In each of the three classes, the average duration of the main and recovery phases defined by the three timings were determined. The timescales and the Dst intensity of each storm were then stretched/contracted according to the average values.

Figure 3 shows the result: Figures 3a and 3b show the average behaviour for moderate and intense magnetic storms, respectively. As expected, the features in the upper panels are nearly identical to what *Loewe and Prölss* [1997] have shown statistically. More precisely, the average diagrams in *Loewe and Prölss* are a mixture of our two diagrams, the upper and lower panels. It should be noted that there is no obvious difference between moderate and intense storms in terms of the overall difference between Types 1 and 2, except for the peak intensities. Note that because the distance between the two peaks in Dst in Type 2 varies from storm to storm, the recovery of the first intensification is not very clear in the superposed plots.

Figures 4a and 4b show the em-responding variations in auroral electrojet activity in AL and in the IMF, respectively. Both quantities consist of the two peaks in

Type 2. This effect is particularly pronounced in the AL plot, where the second peak is more intense than the first. Both Types 1 and 2, peaks in AL and IMF B_z occur well before (> 1 hr) the corresponding peaks in Dst . Also note that the two peaks in B_z are almost equal, but the second AL peak seems to be more intense than the first one. In individual cases, AL often returns to a very quiet state close to zero between the two peaks. However, since the variability of the “quiet” interval between the two Dst minima is quite high, the average “recess” value is finite (nearly -350 nT) in Figure 4a.

4. Discussion

In this paper, we have statistically studied more than 1200 geomagnetic storms. It has been pointed out that the increase in the ring current during the main phase of an intense geomagnetic storm often goes through two steps. This may be surprising because the study of geomagnetic storms has a long history, establishing their average features in which there is the rather simple-looking main phase followed by the slow recovery phase. Assuming this relatively simple picture in mind, the minimum Dst value at the main phase has been utilized as the magnitude of magnetic storms.

4.1. The Intensity of Magnetic Storms

It is natural that when we observe an intense magnetic storm, we assume that something major is occurring at the sun and something intense is traveling through the interplanetary medium to the Earth. The present study clearly demonstrates, however, that it is not always the case in the cause-and-effect relationship of magnetic storms. What really happens is that before a Dst decrease has fully recovered to the pre-storm level, a second decrease tends to follow. In fact, auroral electrojet activity at high latitudes is found to go through two steps as well. The IMF also has a structure of two southward field regions (seen in Figure 4b). This all means that some of the largest geomagnetic storm consists of two or more medium-size storms. Thus, an intense magnetic storm in terms of the peak Dst value may result from a slow decay of the ring current, not from an intense disturbance in the interplanetary fields.

This raises a new exciting question regarding how one can define the intensity of a geomagnetic storm, which has customarily relied on the maximum Dst magnitude observed at the end of the storm main phase. The present study suggests that it is not physically very meaningful to rely on the minimum Dst value to define the storm intensity, particularly for intense magnetic storms. It is interesting to speculate why earlier studies did not notice that an intense magnetic storm goes through two-steps at the main phase. It may well be that studies picked up only the peak value of Dst to identify magnetic storms without paying special attention to how Dst reached the peak. Even though a double structure in the Dst development was found, it might be treated as two magnetic storms, that occurred with a short interval.

4.2. Solar Wind Conditions

The present study indicates that having a large disturbance in the solar wind is not necessary as well as sufficient to generate an intense geomagnetic storm. Our future effort should then be directed toward identifying the cause for a two-stage structure in the southward IMF, not one large southward turning. This structure has in fact been observed in some of the intense magnetic storms [see *Tsurutani et al.*, 1988; 1992; Gonzalez et al., 1989]: see Figure 5 for an example of two-stage development of the main phase. The importance of both sheath (or draped) fields and driver gas fields, carrying southward IMFs, is pointed out by *Tsurutani et al.* [1988] for the generation of major geomagnetic storms, displaying two-stage development characteristics. *Grande et al.* [1996], following this suggestion, have recently shown that CRRES heavy ion charge states were distinctly different during the two injections of the March 1991 great storm. Their interpretation was that these represent ion populations from two different coronal regions, corresponding to sheath and driver gas plasmas.

In connection with a double IMF B_z structure, responsible for Type 2 storms, one important candidate is a shocked B_z field followed by a magnetic cloud field in the interplanetary extension of coronal mass ejections. When the solar ejecta propagates at differential speeds (with respect to the ambient plasma) faster than the magnetosonic speed, a fast forward shock develops ahead of the ejecta. This shock is expected to intensify an ambient B_z field that can exist for some cases and thus originate the first large B_z structure responsible for the first *Dst* enhancement of a Type 2 storm. Then, the internal field of the ejecta itself, often called a magnetic cloud, can show a helical structure with a cross sectional rotation in the Z - X plane, showing a rotation from south to north (or vice versa). The southern part of that field can become the second large B_z structure, responsible for the second stage of a Type 2 storm.

It should be noted that the above scenario applies mainly for solar maximum intervals when CMES are frequent. At solar minimum we expect that high speed streams from coronal holes interacting with slower streams can also produce fairly large B_z structures, especially due to compression of large amplitude Alfvén waves in the corotating interaction region. However, in this latter case a Type 1 storm is expected to be more frequent due to the difficulty in obtaining additional large B_z structures as in the CME case. It is also important to note that the time separation between the B_z structures in the CME case can vary from case to case, leading to a shorter or larger spacing in the corresponding *Dst* enhancements. Finally, when the interplanetary extension of a CME does not involve a shock, and therefore one does not have a shock compressed B_z structure, one could still have a dual B_z structure if the “draping” component (see *Zwan and Wolf*, 1976) ahead the ejecta is large enough.

Correspondingly, if we have both a compressed as well as a draping component, in addition to an internal B_z structure of the ejecta itself, we could expect the development of a magnetic storm consisting of a three-stage growth of the main phase.

4.3. Magnetospheric Processes

As the cause of Type 2 magnetic storms, there are at least two candidate processes in the magnetosphere we need to consider:

1, *Akasofu et al. [1963]* showed that the ring current during a magnetic storm is composed of two parts, most clearly characterized by their decay rates. It was suggested then that one of them must be located closer to the Earth. It might be possible for the two rings to develop differently, making the observed two-stage growth of the ring current. However, the two separate ring current belts cannot account for the rather large separation between the two steps shown in the present statistics.

2. There are two main sources for the ring current: the solar wind origin and the ionospheric component. In particular, the ionospheric component has recently been found to show the largest increase at the inner magnetosphere during the largest magnetic storms [e.g., *Hamilton et al., 1988; Daglis and Alexopoulos, 1996*]. One of the two processes may play essential roles in enhancing one of the two storm-time ring current developments. For example, the first growth in *Dst* may be driven by the steady convection induced by southward IMF [e.g., *Burton et al., 1974; McPherron, 1997*], while the second growth is driven by “fluctuating” electric fields [e.g., *Chen et al., 1994*], resulting from polar substorms. If this is really the case, ionospheric component should dominate in the second development. In other words, the first development tends to prime the ring current, setting up a precondition for the second enhancement by injecting the ring current inward.

In any events, the two-stage development of the ring current results from the existence of two separate IMF B_z intervals. This has been indicated by the results in Figure 4b. However, the interplanetary causes of the two regions have not been fully identified. This will be a topic of an exciting future work in the Space Weather program.

Acknowledgements. We would like to thank L. R. Lyons, S. Kokubun, and L. Bargatze for their illuminating discussion throughout the present study. The work at the Solar-Terrestrial Environment Laboratory was supported in part by the Ministry of Education, Science, Culture and Sports (Monbusho) under a Grant-in-Aid for Scientific Research, Category B. Portions of this work performed at the Jet Propulsion Laboratory,

California Institute of Technology, Pasadena, under contract with the National Aeronautics and Space Administration.

References

- Akasofu, S.-I., The development of geomagnetic storms without a preceding enhancement of the solar plasma pressure, *Planet. Space Sci.*, 13, 297, 1965.
- Akasofu, S.-I., S. Chapman, and D. Venkatesan, The main phase of great magnetic storms, *J. Geophys. Res.*, 68, 3345, 1963.
- Burton, R. K., R. L. McPherron, and C. T. Russell, An empirical relationship between interplanetary conditions and *Dst*, *J. Geophys. Res.*, 80, 4204, 1975.
- Chen, M. W., M. Schulz, and L. R. Lyons, Simulations of phase space distribution of stormtime proton ring current current, *J. Geophys. Res.*, 99, 5745, 1994.
- Daglis, I. A., and W. I. Axford, Fast ionospheric response to enhanced activity in geospace: Ion feeding of the inner magnetotail, *J. Geophys. Res.*, 101, 5047, 1996.
- Dessler, A. J., and E. N. Parker, Hydromagnetic theory of geomagnetic storms, *J. Geophys. Res.*, 64, 2239, 1959.
- Gonzalez, W. D., and B. T. Tsurutani, Criteria of interplanetary parameters causing intense magnetic storms ($Dst < -100$ nT), *Planet. Space Sci.*, 35, 1101, 1987.
- Gonzalez, W. D., B. T. Tsurutani, A. L. Clua de Gonzalez, F. Tang, E. J. Smith, and S.-I. Akasofu, Solar wind-magnetosphere coupling during intense geomagnetic storms (1978 - 1979), *J. Geophys. Res.*, 94, 8835, 1989.
- Grande, M., C. H. Perry, J. B. Blake, M. W. Chen, J. F. Fennell, and B. Wilken, Observations of iron, silicon, and other heavy ions in the geostationary altitude region during late March 1991, *J. Geophys. Res.*, 101, 24707, 1996.
- Hamilton, D. C., G. Gloeckler, F. M. Ipavich, W. Studemann, B. Wilken, and G. Kremser, Ring current development during the great geomagnetic storm of February 1986, *J. Geophys. Res.*, 93, 14343, 1988.
- Joselyn, J. A., and B. T. Tsurutani, geomagnetic sudden impulses and storm sudden commencements, *Eos Trans., AGU*, 71, 1808, 1990.
- Knipp, D., Coordinated study of November 3-4, 1993 magnetic storm, posted on Website, http://www-ssc.igpp.ucla.edu/gcm/event_nov93.html, 1996.
- Loewe, C. A., and G. W. Prölss, Classification and mean behavior of magnetic storms, *J. Geophys. Res.*, 102, in press, 1997. .
- McPherron, R. L., The role of substorms in the generation of magnetic storms, in *Magnetic Storms, Geophys. Monogr. Ser.*, Vol. 98, edited by B. T. Tsurutani, W. Gonzalez, Y. Kamide, and J. K. Alballo, pp. 131-148, American Geophys. Union, Washington, D. C., 1997.

- Sckopke, N., A general relation between the energy of trapped particles and disturbance field near the earth, *J. Geophys. Res.*, 71,3125, 1966.
- Siscoe, G. L., The virial theorem applied to magnetospheric dynamics, *J. Geophys. Res.*, 75,5340, 1970.
- Sugiura, M., and S. Chapman, The average morphology of geomagnetic storms with sudden commencement, *Abhandl. Akad. Wiss. Göttingen. Math. -Phys., Kl. Sonderheft 4*, Gottingen, 1960.
- Taylor, J. R., M. Lester, and T. K. Yeoman, A superposed epoch analysis of geomagnetic storms, *Ann. Geophys.*, 12,612, 1994.
- Tsurutani, B. T., W. D. Gonzalez, F. Tang, S. -I. Akasofu, and E. J. Smith, Solar wind southward B_z features responsible for major magnetic storms of 1978 -1979, *J. Geophys. Res.*, 93, 8519, 1988.
- Tsurutani, B. T., W. D. Gonzalez, F. Tang, and Y. T. Lee, Great magnetic storms, *Geophys. Res. Lett.*, 19,73, 1992.
- Zwan, B. J., and R. A. Wolf, Depletion of the solar wind plasma near a planetary boundary, *J. Geophys. Res.*, 81, 1636, 1976.

Table 1. Classification of geomagnetic storms into two types

	Type 1	Type 2	Uncertain	All
Weak	307	309	37	653
Medium	140	225	34	399
Intense	58	134	8	200
All	505	668	79	12s2

	Type 1	Type 2	Uncertain	All
Weak	47%	47%	<i>6%</i>	100
Medium	35	56	9	100
Intense	29	67	4	100
All	40	53	6	100

Figure Captions

Fig. 1. Schematic representation of Dst for Type 1 and Type 2 geomagnetic storms. See text for parameters that differentiate Type 1 and Type 2 magnetic storms.

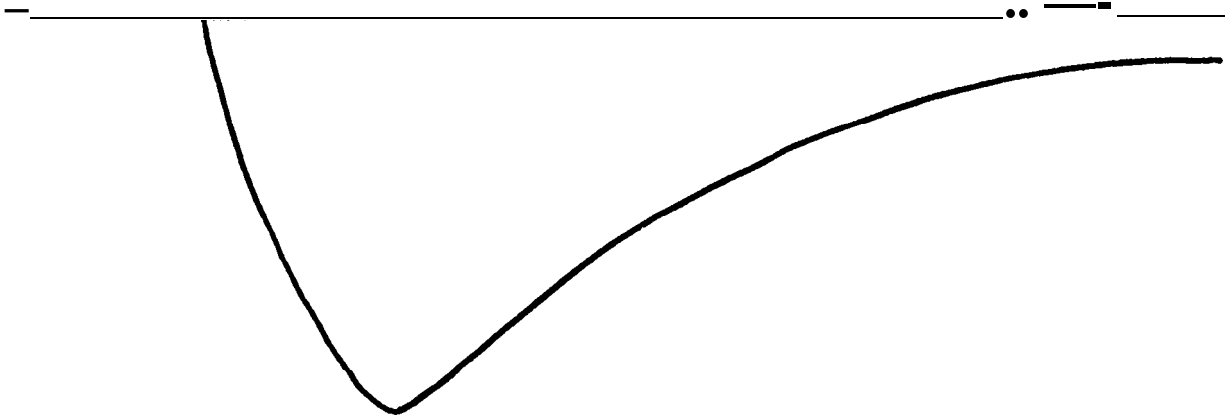
Fig. 2. Typical examples of Type 2 magnetic storms, along with the corresponding B_z component variations in the interplanetary magnetic field.

Fig. 3. Results of a superposed-epoch analysis of Dst for Type 1 and Type 2 magnetic storms: (a) moderate, and (b) intense magnetic storms.

Fig. 4. Results of a superposed-epoch analysis of (a) the AL index, and (b) the IMF B_z component for Type 1 and Type 2 magnetic storms,

Fig. 5. An example of Type 2 magnetic storms from an earlier publication [Gonzalez and Tsurutani, 1987]. The solar wind speed was nearly constant throughout the magnetic storm, but the interplanetary magnetic field had clear two southward turnings (hatched),

Type 1



Type 2

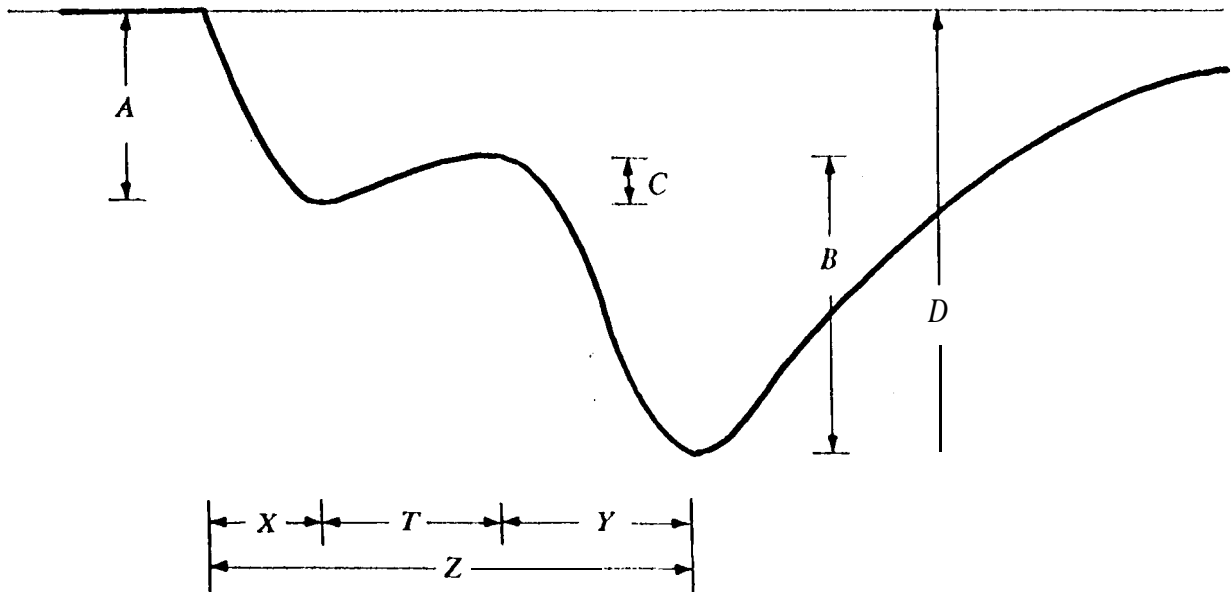
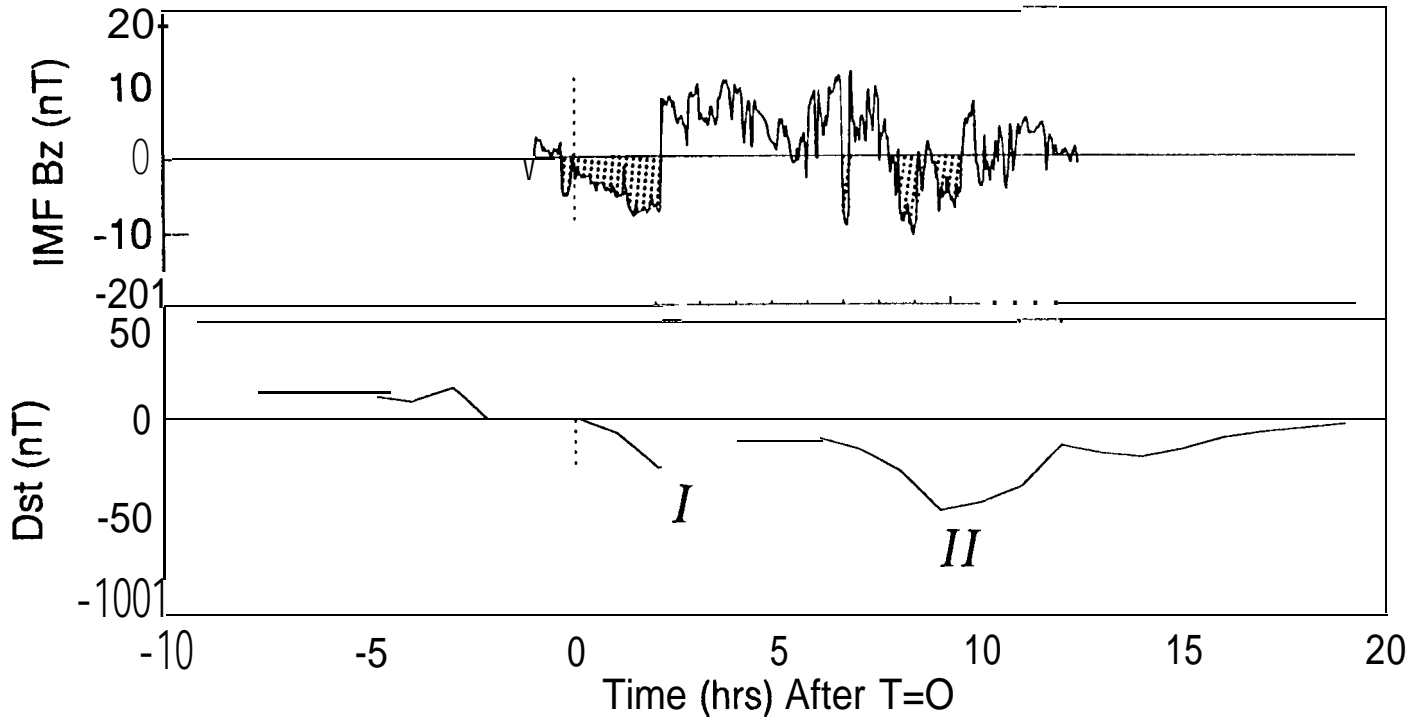


Figure 1

November 13, 1985



May 5, 1989

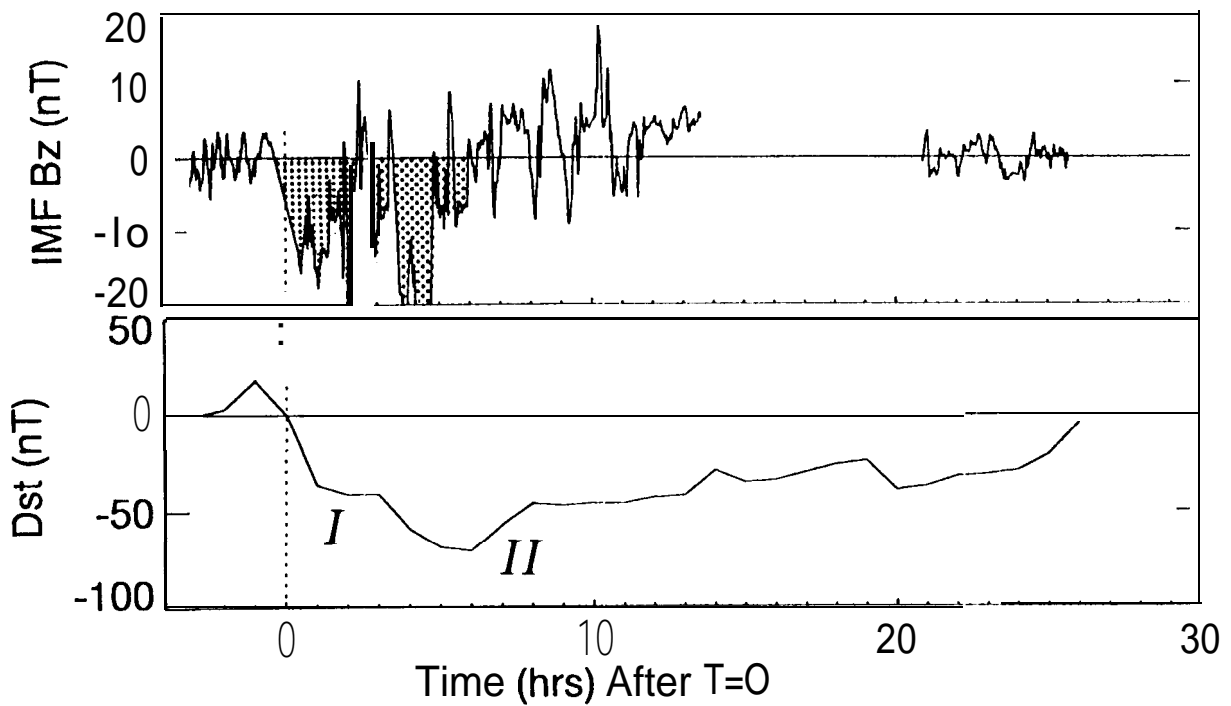


Figure 2

Moderate storms

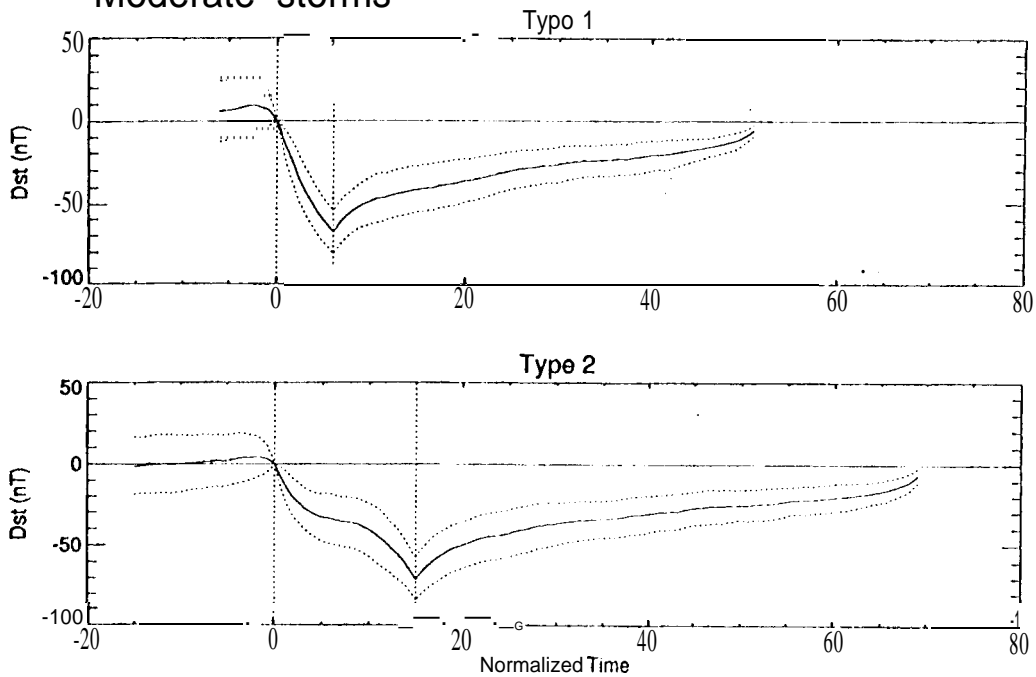


Figure 3a

Intense storms

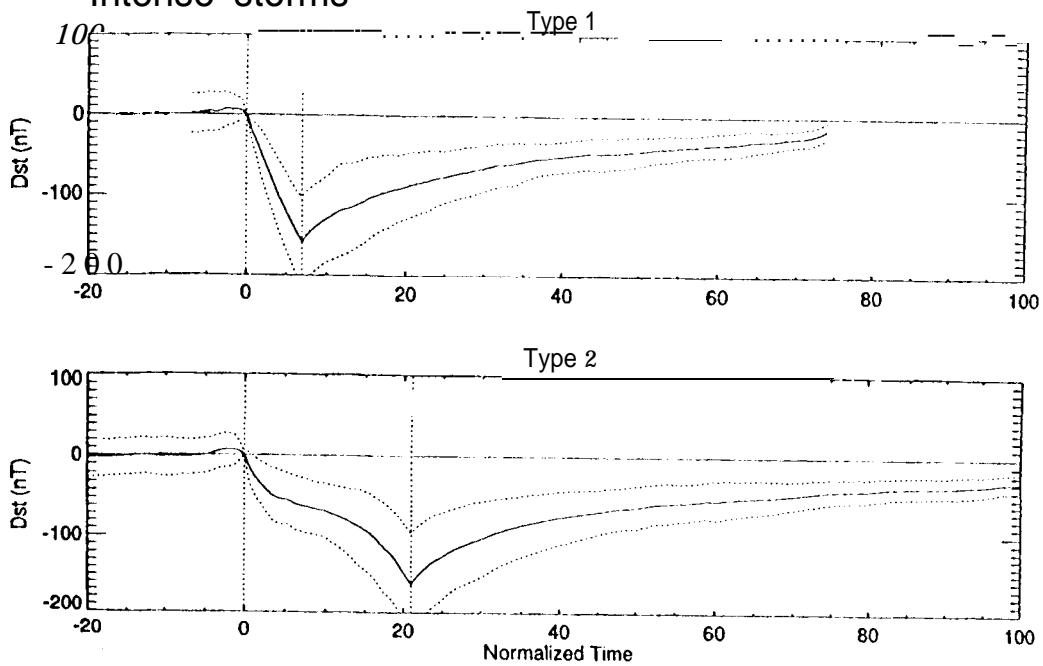


Figure 3b

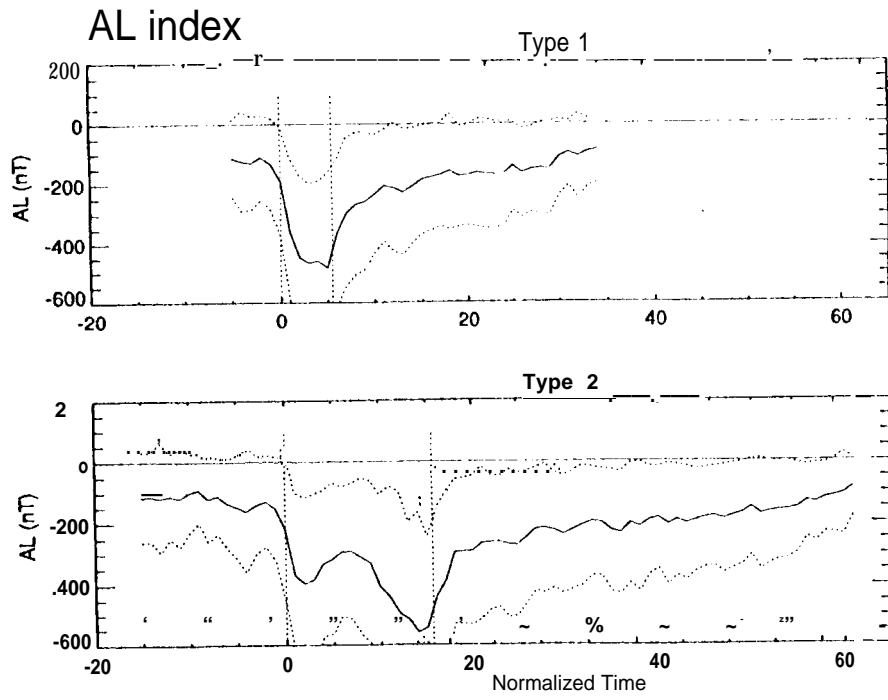


Figure 4a

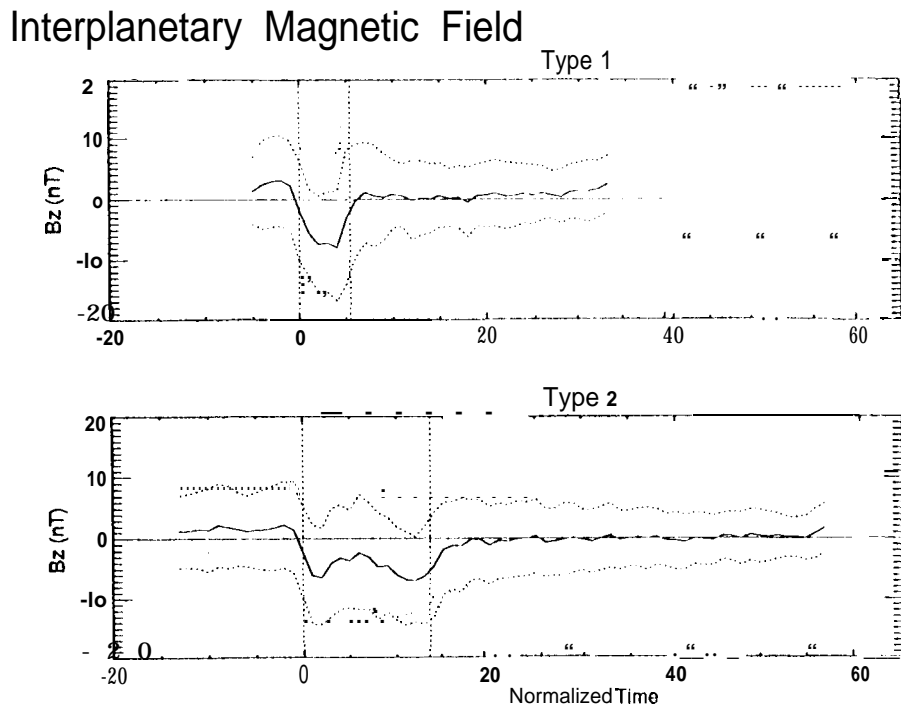


Figure 4b

Figure 5

